npj | climate and atmospheric science

www.nature.com/npjclimatsci

ARTICLE OPEN

Check for updates

Distinct decadal modulation of Atlantic-Niño influence on ENSO

Jae-Heung Park[1]✉, Jong-Seong Kug[1,2]✉, Young-Min Yang[3,4], Mi-Kyung Sung[5], Sunyong Kim[6], Hyo-Jeong Kim[7], Hyo-Jin Park[8] and Soon-Il An[1,8]

It is known that winter Atlantic-Niño events can induce the El Niño–Southern oscillation (ENSO) in the following winter with a lag of 1-year during one period. On the other hand, summer Atlantic-Niño events can lead to the ENSO in the subsequent winter with a half-year lag during another period. In this study, we investigate the distinct interdecadal modulation of the effect of the Atlantic-Niños on ENSO by analyzing observational reanalysis datasets. During the mid-twentieth century, the winter Atlantic-Niño exhibited increased intensity and extended westward due to warmer conditions in the tropical western Atlantic. As a result, convection occurred from the Amazon to the Atlantic, triggering an atmospheric teleconnection that led to trade wind discharging and equatorial Kelvin waves, ultimately contributing to the development of ENSO. In contrast, during late twentieth century, summer Atlantic-Niño events were closely linked to the South America low-level jet in boreal spring. This connection led to the formation of widespread and intense convection over the Amazon to the Atlantic region. Then, the Walker circulation was effectively modulated, subsequently triggering ENSO events. Further analysis revealed that the interdecadal modulation of the Atlantic–South America–Pacific mean state plays a crucial role in shaping the impact of Atlantic-Niños on ENSO by modifying not only the characteristics of the Atlantic-Niños but also ocean–atmospheric feedback process. Therefore, improving our understanding of the interdecadal modulation of the climatological mean state over the Pacific to Atlantic regions enables better anticipation of the interaction between the Atlantic and Pacific Oceans.

npj Climate and Atmospheric Science (2023)6:105 ; https://doi.org/10.1038/s41612-023-00429-9

INTRODUCTION

The tropical Atlantic Ocean exhibits a wide range of climate variability patterns and exerts a significant influence on local weather and climate, spanning across the African and American continents[1–3]. Its impact also extends to remote regions such as the North Atlantic, Europe, Indian Ocean, and the Pacific Ocean[4–7]. Among the various variability modes of sea surface temperature (SST) anomaly (SSTA) in the tropical Atlantic, one prominent mode is the Atlantic-Niño[7–12]. The development of Atlantic-Niño is attributed to internal processes, particularly the Bjerknes feedback[10,13,14], which demonstrates a positive feedback loop between the ocean and atmospheric based on the thermocline slope. Additionally, external forcings from the South and North Atlantic[15–18] and Indian Oceans[19] can contribute to the evolution of Atlantic-Niño events.

The Atlantic-Niño exhibits its maximum variability during the boreal summer[20] (for convenience, seasons denoted in this study follow those in the Northern Hemisphere). In contrast, the maximum variability of El Niño–Southern Oscillation (ENSO) occurs during winter[21]. Concerning the lead-lagged relationship between the Atlantic-Niño and ENSO, it is widely recognized that the warm (cold) phase of the summer Atlantic-Niño enhances the likelihood of occurrence of La Niña (El Niño) events in the following winter[22–27].

An often overlooked aspect of the Atlantic-Niño is that it has a second peak during winter[28]. This secondary peak is also based on the presence of a shallow thermocline along the equatorial eastern Atlantic between October and December. The shallow thermocline creates favorable conditions for the thermocline feedback, thereby contributing to the development of winter Atlantic-Niño. Recent reports have indicated that, similar to the summer Atlantic-Niño, the winter Atlantic-Niño can also trigger ENSO events with a lag of 1-year[29].

Notably, the effects of the summer and winter Atlantic-Niños on ENSO development are not stationary[23,29–31]. Specifically, the influence of the summer Atlantic-Niño on ENSO has intensified since the mid-twentieth century, particularly after the 1980s[23,30,31]. Previous studies have attributed this strengthening effect to the westward expansion of the Atlantic-Niño and its associated convective precipitation[30–32]. The changes in the summer Atlantic-Niño characteristics and its impact have been linked to the long-term natural variability (e.g., Atlantic Multidecadal Oscillation (AMO))[32,33]. It has also been reported that the position of the Atlantic intertropical convergence zone (ITCZ), associated to the South Atlantic warming/cooling, determines the characteristics of the summer Atlantic-Niño and that the Indian Ocean plays a role in transmitting the summer Atlantic-Niño effect to the equatorial Pacific[30,31]. Similarly, the effect of the winter Atlantic-

[1]Division of Environmental Science and Engineering, Pohang University of Science and Technology (POSTECH), Pohang, South Korea. [2]Institute for Convergence Research and Education in Advanced Technology, Yonsei University, Seoul, South Korea. [3]Key Laboratory of Meteorological Disaster, Ministry of Education (KLME)/Joint International Research Laboratory of Climate and Environment Change (ILCEC)/Collaborative Innovation Center on Forecast and Evaluation of Meteorological Disasters (CIC-FEMD), Nanjing University of Information Science and Technology, 210044 Nanjing, China. [4]State Key Laboratory of Numerical Modeling for Atmospheric Sciences and Geophysical Fluid Dynamics, Institute of Atmospheric Physics, Chinese Academy of Sciences, 100029 Beijing, China. [5]Center for Sustainable Environment Research, Korea Institute of Science and Technology, Seoul, Korea. [6]Climate Analytics Department, APEC Climate Center, Busan, South Korea. [7]Low-Carbon and Climate Impact Research Centre, School of Energy and Environment, City University of Hong Kong, Tat Chee Ave, Kowloon Tong, Hong Kong, People's Republic of China. [8]Department of Atmospheric Sciences/Irreversible Climate Change Research Center, Yonsei University, Seoul, South Korea. ✉email: jhp11010@gmail.com; jskug1@gmail.com

Niño on ENSO was found to be enhanced during the mid-twentieth century[29] although the underlying processes have not been thoroughly investigated.

While progress has been made in understanding the influence of the Atlantic on the Pacific[34–38], there is still a need for a comprehensive examination of its non-stationary nature. Specifically, it is necessary to investigate how the lead-time of the Atlantic-Niño effect on ENSO is determined over interdecadal timescales. Moreover, since the impact of the winter Atlantic-Niño on ENSO has only recently been reported[29], further investigation into this process is warranted. Therefore, in this study we aim to explore the observed interdecadal modulation of the Atlantic-Niño effect on ENSO, with a particular focus on its lead time from the perspective of long-term natural variability. Our analysis will demonstrate that the interdecadal modulation of the climatological mean state across the Atlantic to Pacific Oceans not only alters the characteristics of the Atlantic-Niño but also influences feedback processes. This collective modification plays a crucial role in determining the lead time of the Atlantic-Niño effect on ENSO.

RESULTS

Interdecadal modulation of the relationship between the Atlantic-Niño and ENSO

To access the interdecadal modulation of relationships between the Atlantic-Niño and ENSO, we first performed a lead-lagged correlation analysis between the monthly Atlantic-Niño and Niño-3.4 indices (indices are described in the "Method" section). This analysis was carried out using a 300-month (25-year) running window, wherein climatological mean of each index was first subtracted, and the trend within each analyzed period was removed. For instance, when conducting a correlation analysis over 1901–1925, the trend during that period was eliminated. In Fig. 1a, the correlation coefficients for negative lags on the *x*-axis are found to be positive overall, indicating a positive lead of ENSO on the Atlantic-Niño. However, these results were generally insignificant, indicating a limited influence of ENSO on the Atlantic-Niño during the twentieth century. This limited influence can be attributed to the complex interactions among various oceanic and atmospheric processes in the tropical Atlantic, which are induced by ENSO[39,40].

In contrast, significant negative correlations in positive lags on the x-axis demonstrate that the Atlantic-Niño has had a notable impact on ENSO throughout the same period. The time lag involved in this relationship has displayed considerable variability. Specifically, the Atlantic-Niño typically led ENSO by less than 9 months (indicated by the right black vertical dotted line in Fig. 1a) during the early and late twentieth century, whereas lag times of over 9 months were observed around the 1870s (weak signals) and in the mid-twentieth century. Given the negative correlation at these time lags, our findings suggest that warming (cooling) over the Atlantic-Niño region promoted the development of La Niña (El Niño) events with an approximately half-year lead during the early and late twentieth century. In contrast, during the mid-twentieth century, the Atlantic-Niño contributed to the ENSO development approximately with a lag of 1-year.

These findings are consistent with a previous study[29] (Hounsou-Gbo et al. 2020; their Fig. 2); however, the underlying mechanism responsible for interdecadal modulation of Atlantic-Niño effects on ENSO remains to be elucidated. To gain further insight into this modulation, we focused on the three specific periods with a criterion of a 9-month lead time; 1890–1925, 1940–1975, and 1980–2015. Subsequently, we subdivided the correlation analysis by calendar month to determine the lag time by which the Atlantic-Niño (y-axis) leads ENSO at each month during these subperiods (Fig. 1b–d). For the 1890–1925 period (Fig. 1c), the strongest signals were observed during the summer season (June–August) with a lag time of 0–7 months. This suggests that summer Atlantic-Niño warming events were followed by La Niña events in the following winter. Similarly, for the 1980–2015 period (Fig. 1b), the summer Atlantic-Niño significantly led La Niña events with comparable lag times. While winter and spring showed sporadic and weaker negative correlations with Atlantic-Niño events during this period, the summer signals were more pronounced and significant.

In contrast, during the period 1940–1975, the most robust correlation was observed for winter with approximately a lag of 1-year (6–15-month) (Fig. 1d). This finding clearly indicates that winter Atlantic-Niño warming can trigger a La Niña event with a longer lead time of 1-year during specific decades. A similar pattern to the mid-twentieth century (as shown in Fig. 1a) was observed for the period before the 1880s; however, we did not present detailed seasonal lags due to the short time span and lower significance of that period.

The observed recurring changes in lag may imply that slowly evolving background conditions play a modulating role in transmitting the influence of the Atlantic-Niño to the Pacific. In the subsequent analysis, we further examine the mechanisms through which summer (JJA) and winter (DJF) Atlantic-Niño events can trigger ENSO events with distinct short- and long-term leads, respectively.

Summer Atlantic Niño effects: 1940–1975 versus 1980–2015

To gain insight into the underlying dynamics contributing to the observed changes in lag scales, we now investigate the spatiotemporal evolution of ENSO events associated with Atlantic-Niño events during each subperiod. We focus on the two recent periods of 1940–1975 and 1980–2015, as they exhibit significant differences. It is worth mentioning that the Atlantic-Niño effect on ENSO for 1890–1925 is generally comparable to that observed in the 1980–2015 period, as inferred from the results in Fig. 1 (please also refer to the Supplementary Fig. 1).

Figure 2a depicts the anomalous patterns of SST, sea level pressure (SLP), low-level wind, and precipitation regressed on the summer Atlantic-Niño index during the 1940–1975 period. In AMJ[1] (where [1] represents the corresponding year of a summer Atlantic-Niño event), a SSTA warming was observed from the equatorial central Atlantic to the Benguela-Niño area, accompanied by westerly wind and positive precipitation anomalies (for other seasons, please refer to Supplementary Fig. 2). Notably, negative precipitation anomalies were also observed over the equatorial northwestern Atlantic (indicated by orange dots around 50°W, 5°N), resulting in the formation of an anomalous precipitation dipole over the equatorial Atlantic. This precipitation dipole, however, is unfavorable to significantly alter the Walker circulation between the Atlantic to Pacific regions[41] (illustrated in Supplementary Fig. 3). Consequently, under these conditions, it becomes challenging for ENSO to initiate.

The westerly wind anomalies during spring cause further equatorial Atlantic warming through the Bjerknes feedback mechanism, leading to its peak phase during summer (JJA[1]). However, in such cases, the SSTA warming and precipitation remain confined to the central to eastern equatorial Atlantic and do not reach the eastern coast of South America. As a result, the atmospheric teleconnection toward the Pacific is insignificant. Therefore, signals associated with the summer Atlantic-Niño events are rarely observed outside of the Atlantic, particularly in the tropical Pacific. This result aligns with the lead-lagged correlation analysis depicted in Fig. 1a, d and signifies a negligible effect of the summer Atlantic-Niño on the tropical Pacific.

Moving on to the period 1980–2015, we examined the impact of summer Atlantic-Niño events on ENSO. Figure 2b represents the lead-lagged influence of the summer Atlantic-Niño during this

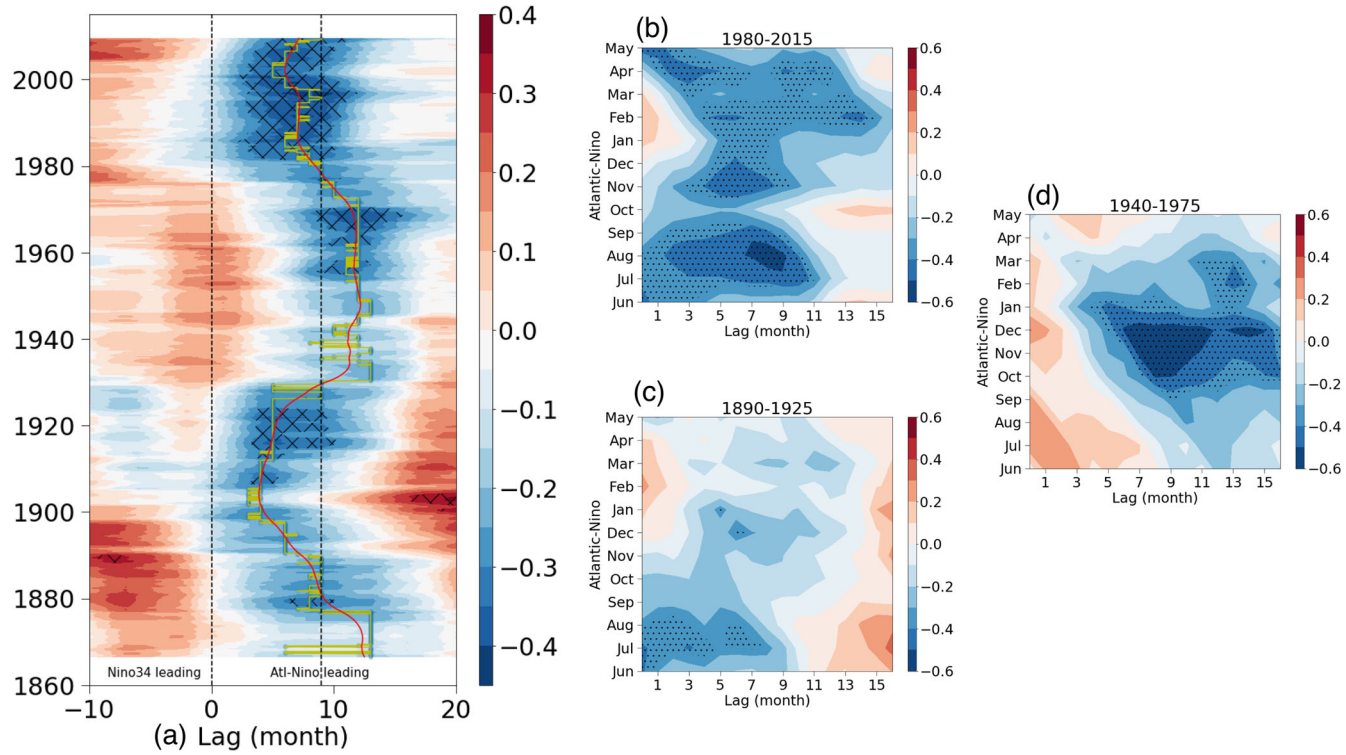

Fig. 1 Interdecadal modulation of the relationship between Atlantic-Niño and ENSO. a 300-month (25-year) running lead-lagged correlation coefficients between the Niño-3.4 and Atlantic-Niño indices for the period 1854–2020 (*y*-axis). Negative and positive values on the *x*-axis indicate leads of Niño3.4 and the Atlantic-Niño at monthly timescales, respectively. The left vertical black dotted line indicates the simultaneous relationship and the right vertical black dotted line denotes the nine-month lead of the Atlantic-Niño relative to ENSO, dividing the regimes into short- and long-lead periods. Hatching indicates values above 0.3 at a 95% confidence level using a two-tailed Student's *t*-test with a degree of freedom of 40. The yellow line indicates the number of months for which the Atlantic-Niño leads ENSO by tracing the lead month corresponding to the maximum negative correlation value, while the red line illustrates its low-pass filter (120-month) termed the Atlantic-Niño lead time index. **b** Lagged correlation between the Atlantic-Niño and ENSO indices for the period 1980–2015, where the *x*-axis indicates the number of months by which the Atlantic-Niño index leads the Niño-3.4 index; the *y*-axis indicates the period of June to the following May. The negative maximum is found at 0–6 (*x*-axis) during July (*y*-axis), indicating that the Atlantic Niño in July negatively leads ENSO with a lag of 0–6 months. Hatching indicates the 95% confidence level using a two-tailed Student's *t*-test. **c**, **d** Similar to **b**, but for the periods of 1890–1925 and 1940–1975, respectively.

period. In AMJ[1], equatorial Atlantic warming is observed, accompanied by anomalous westerly wind and increased precipitation. Unlike the period 1940–1975, the SSTA warming extends westward towards South America without negative precipitation anomalies in the equatorial northwestern Atlantic (Supplementary Fig. 4). Particularly, there are notable precipitation anomalies over the Amazon in the tropical South America, indicating enhanced convection (Supplementary Fig. 5), and therefore a strong atmospheric teleconnection toward the Pacific (Supplementary Fig. 3). Consequently, easterly wind anomalies with weak SSTA cooling occur over the equatorial central Pacific, initiating La Niña events.

During AMJ[1], in addition to the westerly wind anomalies over the equatorial western Atlantic, strong meridional wind anomalies over the south-central South America (around La Plata basin) to the tropical South America are observed. These meridional winds, along with the Andes mountains, correspond to the South America low-level jet (SALLJ)[42–45]. The SALLJ is quantified as the averaged meridional wind at 850 hPa over the 55–65°W and 15–25°N (for the SALLJ index, please refer to Method and Supplementary Fig. 6). Note that the SALLJ is northerly all year long. We have discovered that the variability of the SALLJ during AMJ[1] significantly precedes both Amazon precipitation (MJJ[1]) and the Atlantic-Niño (JJA[1]) by a lag of 1- and 2-month during this period, respectively (Supplementary Table 1).

Based on these findings, we conducted a lead-lagged correlation analysis between the SALLJ index (AMJ[1]) and the summer Atlantic-Niño index (JJA[1]) using a 30-year running window (Fig. 3a). Note that the trend within each 30-year window is removed from both indices. The correlation coefficient exhibits an increasing trend since the 1940s and reaches ~0.7 around 2000s, indicating a significant connection between SALLJ and summer Atlantic-Niño during recent decades.

Figure 3b–e depict the spatial patterns of low-level wind, low-level divergence, precipitation, and specific humidity regressed onto the SALLJ during both periods. During 1940–1975 (Fig. 3b, c), SALLJ remains confined to the subtropical to mid-latitude regions, giving rise to a precipitation dipole between the La Plata basin and southeastern Brazil. In contrast, during the period 1980–2015 (Fig. 3d, e), the SALLJ extends further into the Amazon region, penetrating through the tropics to mid-latitudes. Consequently, the SALLJ accompanies a meridionally broad dipole structure of low-level divergence and specific humidity between the tropics and mid-latitudes. This result indicates that the SALLJ transports moisture to the Amazon and equatorial Atlantic, and the associated low-level divergence triggers convection. As a result, as SALLJ links to the summer Atlantic-Niño (Fig. 3a), enhanced precipitation anomalies occur over the Amazon to equatorial Atlantic.

To summarize, the summer Atlantic-Niño combined with SALLJ triggers strong convection from the Amazon to the equatorial Atlantic, establishing a persistent Walker circulation (Supplementary Fig. 3). This circulation induces easterly wind anomalies with negative precipitation anomalies, leading to SSTA cooling along

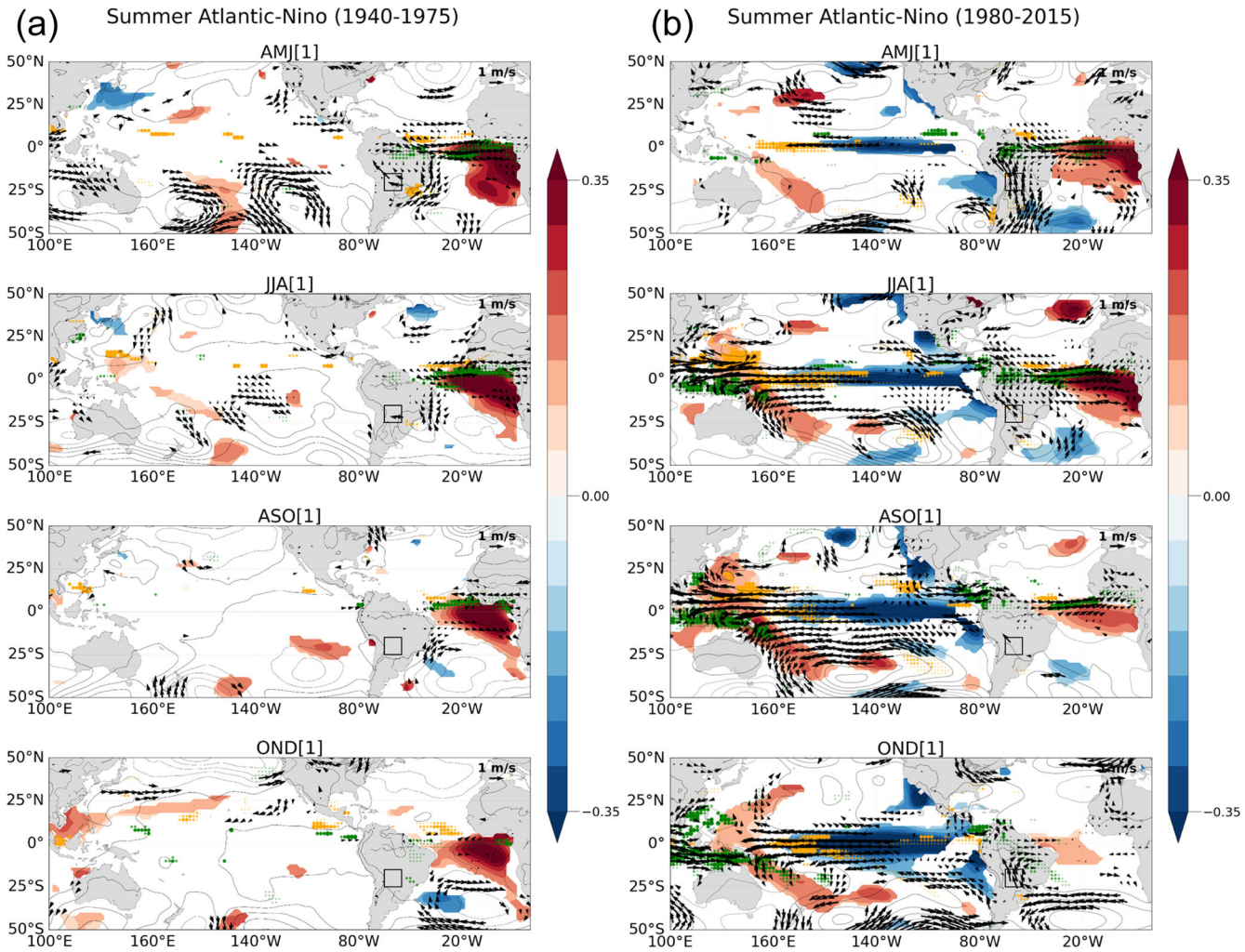

Fig. 2 Effects of Summer Atlantic-Niño on the following ENSO. a Regressed SSTA (shading, °C, shading bar shown at right), SLPA (contour, 0.5 hPa), low-level wind anomaly (vector, at 850 hPa), and precipitation anomaly (dots; green and orange for positive and negative, respectively) against the June–July–August (JJA) Atlantic-Niño index for the period 1940–1975. Top to bottom panels correspond to the April–May-June (AMJ) mean, JJA mean, August–September–October (ASO) mean, and October–November–December (OND) mean, respectively. Anomalous SST, winds, and precipitation are marked with a 95% confidence level when the Student's *t*-test is satisfied (df = N-2). **b** Same as **a**, but for the period 1980–2015.

the equatorial Pacific. From JJA[1] to D[1]JF[2] (Fig. 2 and Supplementary Fig. 2), the equatorial Atlantic SSTA warming decays, while the positive Bjerknes feedback in the Pacific results in the occurrence of La Niña events.

Winter Atlantic-Niño effects: 1940–1975 *versus* 1980–2015

Figure 4a shows the lagged influence of the winter Atlantic-Niño during the period 1940–1975. In D[0]JF[1], the winter Atlantic-Niño exhibits significant development with anomalous westerly winds. Simultaneously, there are strong cyclonic convergent flows with moisture toward the Amazon and equatorial western Atlantic from both hemispheres (Supplementary Fig. 7), accompanied by enhanced precipitation over the region. As a result, the atmospheric features associated with winter Atlantic-Niño events during the period 1940–1975 are shifted towards the South America (Fig. 4b and Supplementary Figs. 4 and 5). The westward displacement of precipitation induced by the winter Atlantic-Niño suggests an effective atmospheric teleconnection toward the Pacific Ocean.

Winter Atlantic-Niño related warming and precipitation persist until MAM[1], resulting in the maintenance of an atmospheric teleconnection toward the Pacific. The northeasterly wind anomalies observed over the off-equatorial North Pacific in D[0]JF[1] extend equatorward from winter to spring (for other seasons, please refer to Supplementary Fig. 9). These easterly wind anomalies along the equatorial Pacific generate oceanic upwelling Kelvin waves, initiating a La Niña event. Concurrently, the meridional expansion of northeasterly winds is associated with a stronger positive wind stress curl and increased trade-wind discharge (Supplementary Fig. 8). Over the northern region of the northeasterly wind anomalies, subtropical North Pacific highs becomes prominent. The correlation coefficient between the winter Atlantic-Niño and the subtropical North Pacific high from winter to spring (120–180°W, 5–30°N) reaches a 95% confidence level (0.5), indicating a close relationship between the subtropical North Pacific and the Atlantic Oceans.

From spring (MAM[1]) to winter (D[1]JF[2]), the winter Atlantic-Niño related warming diminishes, but the Bjerknes feedback in the Pacific develops a La Niña event. Equatorial easterly wind anomalies are observed in the western to central equatorial Pacific, but they do not extend to the far eastern equatorial Pacific, implying an increased likelihood of Central Pacific (CP)-type ENSO formation[46–48].

Next, we investigated the winter Atlantic-Niño effect on the tropical Pacific during the period 1980–2015 (Fig. 4b). In D[0]JF[1],

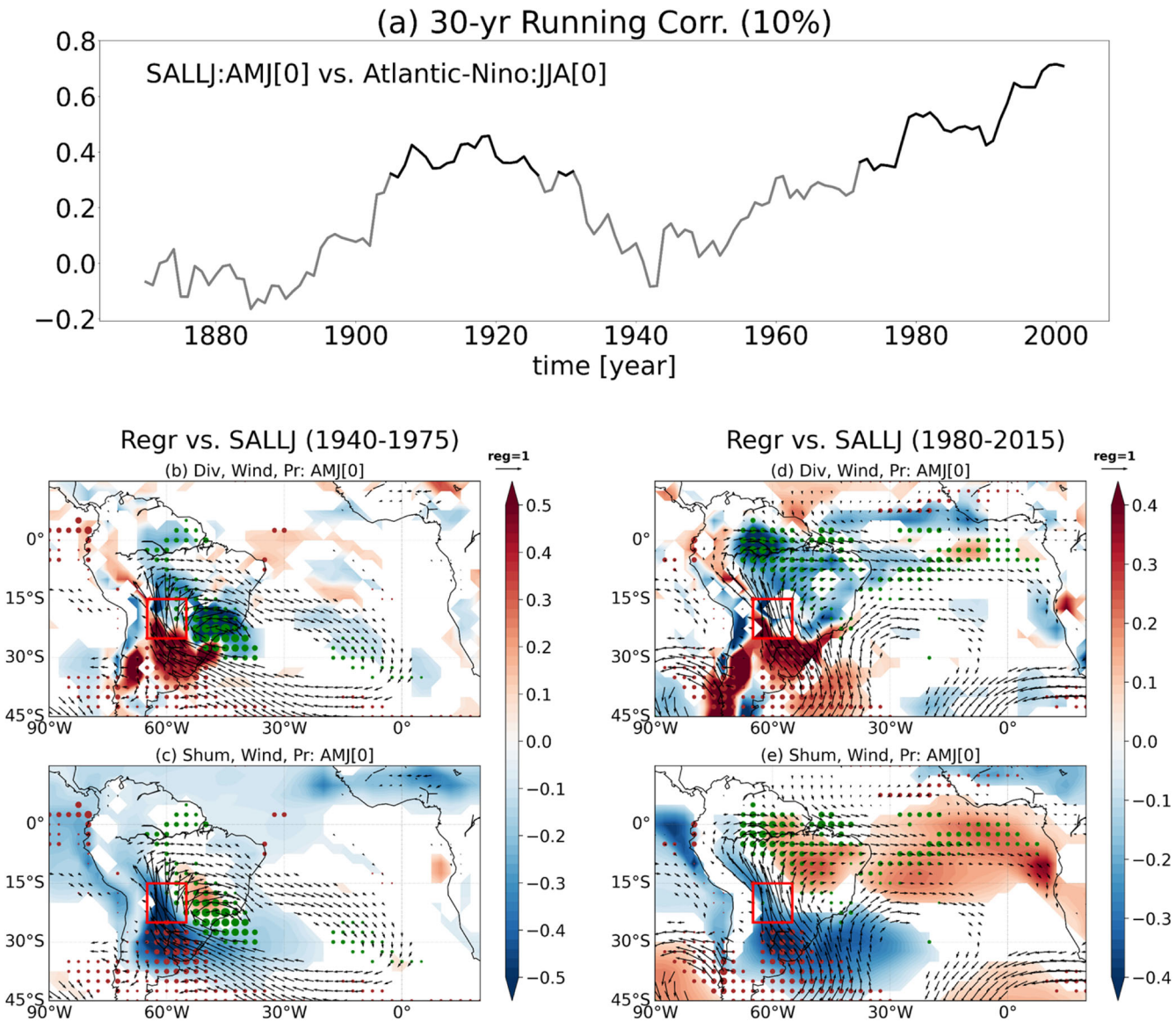

Fig. 3 Interdecadal modulation of the relationship between SALLJ and Summer Atlantic-Niño. a 30-year running correlation coefficients between the SALLJ (AMJ, v, 55–65°E, 15–25°S) and Atlantic-Niño (JJA) indices, wherein a trend within each 30-year window is removed from both indices. Black line indicates a 90% confidence level. **b** Regressed low-level divergence (shading), low-level wind (vectors, 850hPa, 90% confidence level), and precipitation (dots, green/brown for positive/negative, 90% confidence level) in AMJ onto SALLJ index (AMJ) during 1940–1975. Herein, red box indicated the region of SALLJ. **c** Same as **b**, but low-level divergence is replaced into specific humidity. **d**, **e** Same as **b**, **c**, but during 1980–2015.

there is a SSTA warming accompanied by westerly wind anomalies in the central equatorial Atlantic. However, precipitation and wind anomalies associated with Atlantic-Niño events during this period are weaker and displaced eastward compared to those observed in the 1940–1975 (Supplementary Figs. 4, 5, 10, and 11). Moreover, another area of SSTA warming emerges near northeastern Brazil in the southern hemisphere, accompanied by northwesterly wind anomalies that cross the equator in JFM[1] (Supplementary Fig. 9). As a result, the winter precipitation responses along the equatorial Atlantic are not well-organized, making it more difficult to establish effective atmospheric teleconnections towards the Pacific.

The Atlantic-Niño persists until MAM[1]. Simultaneously, the SALLJ is strong, which induces convergent atmospheric flows and significant precipitation in the Amazon region, generating an atmospheric teleconnection. Consequently, easterly wind anomalies occur over the equatorial Pacific in MAM[1], leading to SSTA cooling along the equatorial Pacific in JJA[1]. However, the limited development of SSTA cooling entails that La Niña formation is not apparent in D[1]JF[2]. We attribute this weak SSTA cooling to the weak atmospheric teleconnection resulting from the weak and eastward-displaced Atlantic-Niño and the absence of trade wind discharge in previous winter (D[0]JF[1]).

The role of interdecadal climatological mean state change in the lead time of the Atlantic-Niño and its effects on ENSO

In this section, we aim to identify the factors that determine the length of the lead time of the Atlantic-Niño effect on ENSO, taking into account the long-term modulation of the climatological mean state. To achieve this, we first obtained time series indicating how many months Atlantic-Niño leads ENSO; this was determined by tracing the lead month corresponding to the maximum negative correlation value, represented by the yellow line in Fig. 1a.

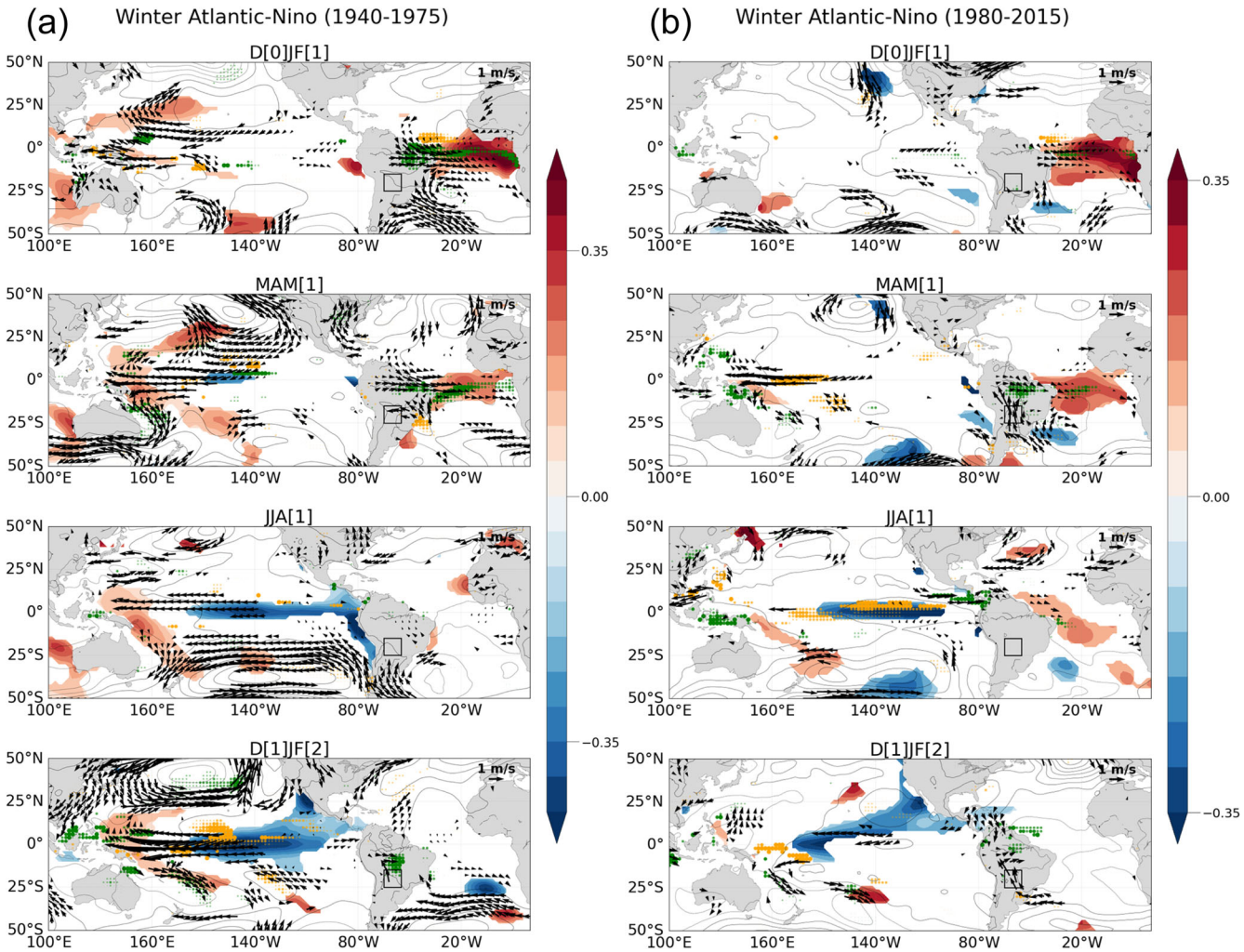

Fig. 4 Effects of winter Atlantic-Niño on the following ENSO. a Regressed SSTA (shading, °C, shading bar shown at right), SLPA (contour, 0.5 hPa), low-level wind anomaly (vector, at 850 hPa), and precipitation anomaly (dots; green and orange for positive and negative) against the December–January–February (DJF) Atlantic-Niño index during the period 1940–1975. Top to bottom panels correspond to the DJF mean, March–April–May (MAM) mean, June–July–August (JJA) mean, and following DJF mean, respectively. Anomalous SST, winds, and precipitation are marked when a 95% confidence level by Student's *t*-test is satisfied (df = N-2). **b** same as **a**, but for the period 1980–2015.

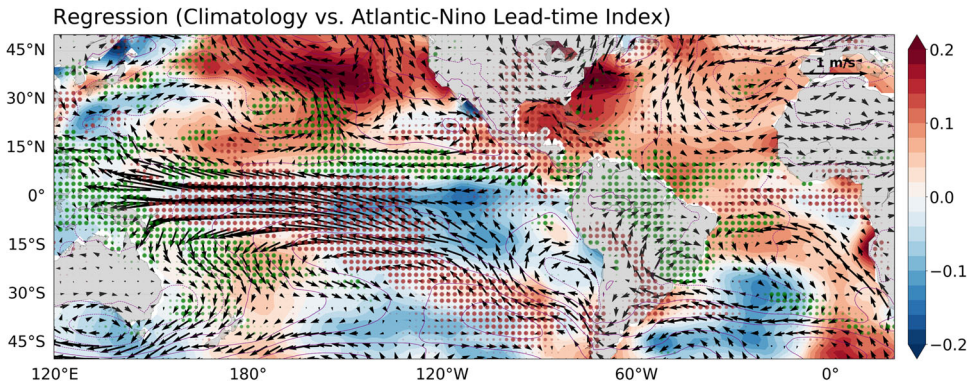

Fig. 5 Atlantic-Niño lead-time associated climatological mean state. Long-term (300-month) climatological mean SST (shading), low-level wind (vectors), precipitation (green and brown dots for positive and negative), and SLPA (contour) regressed onto the Atlantic-Niño lead-time index for the period 1885–2015 indicated as a red curve in Fig. 1a.

Subsequently, the time series was smoothed by applying a low-pass filter (120-month), which is termed the Atlantic-Niño lead-time index (red line in Fig. 1a). Figure 5 shows a regression map of climatological (25-year) mean SST, low-level wind, and precipitation against the Atlantic-Niño lead time index over the last century. Note that this result is comparable to the difference of seasonal (JJA, DJF) climatological mean state between 1940–1975 and 1980–2015 (Supplementary Fig. 12). It is

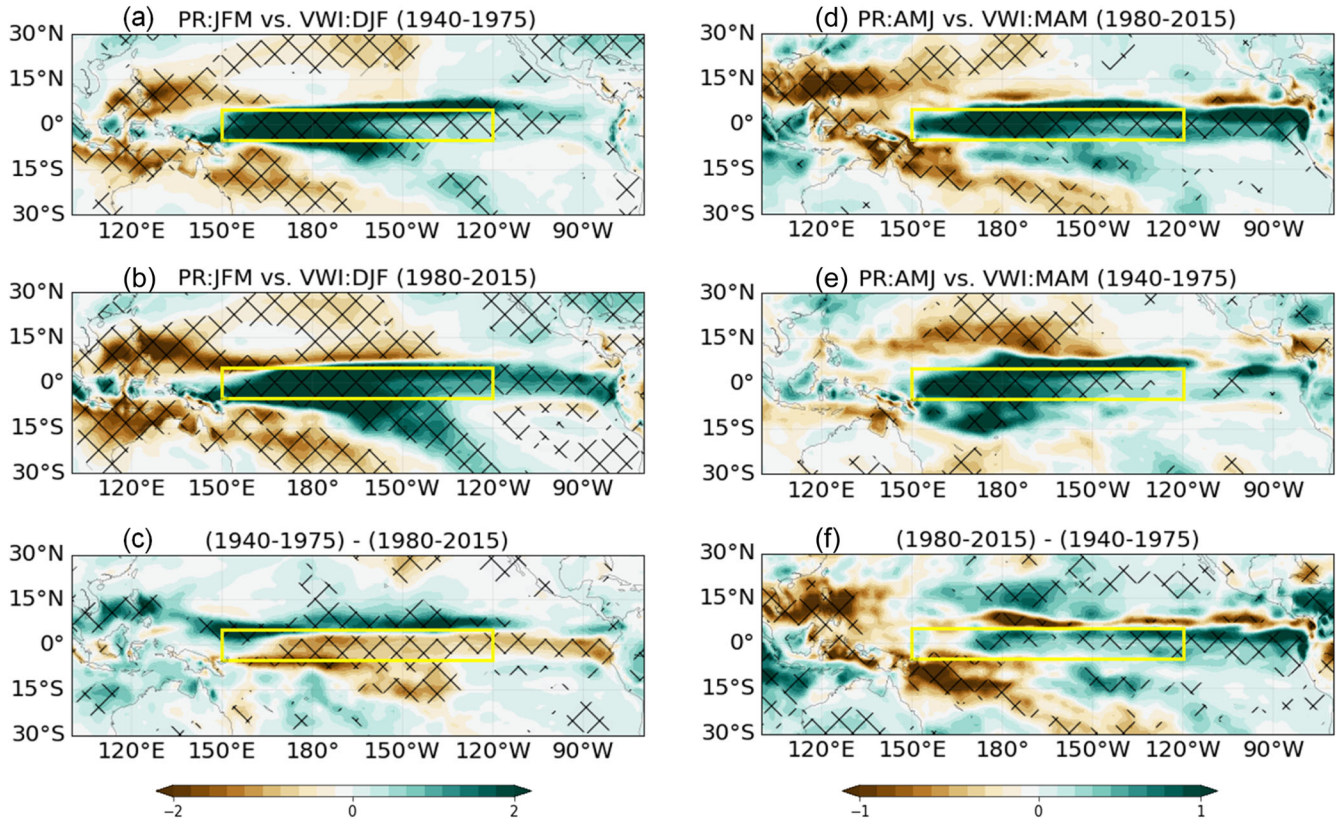

Fig. 6 Precipitation response to the vertical motion of the equatorial Pacific. a Regressed precipitation anomaly in January–February–March (shading bar shown at the bottom) against the vertical wind index (VWI, obtained by multiplying the areal-averaged omega at 500hPa over the 150°E–120°W and 5°S–5°N by −1, indicated by a yellow rectangle) in March–April–May (MAM) during the period 1940–1975. **b** Similar to **a**, but for the period 1980–2015. **c** (**a**) minus (**b**). **d**–**f** Same as **a**–**c**, but for the regressed precipitation anomaly in JFM against VWI in December–January–February (DJF) during (**d**) 1980–2015, (**e**) 1940–1975, and (**f**) the difference between the two.

demonstrated that, during the period when the Atlantic-Niño leads ENSO with a long lead-time (e.g., 1940–1975), tropical western Atlantic warming with increased precipitation and equatorial eastern Pacific cooling with stronger easterly wind and precipitation reduction are prevalent. Concurrently, the Atlantic ITCZ and South Atlantic Convergence Zone (SACZ) get intensified with southerly mean wind over the central South America (i.e., weakened SALLJ). Conversely, during the period when the Atlantic-Niño leads ENSO with a short lead time, the climatological mean state exhibits the opposite characteristics (e.g., 1980–2015).

Winter Atlantic-Niño effect on ENSO under tropical western Atlantic warming and eastern equatorial Pacific cooling mean state (1940–1975)

When the Atlantic-Niño leads ENSO with a long lead time (1940–1975) (Fig. 5), the tropical western Atlantic is warm and humid (i.e., high moist enthalpy), compared to the tropical eastern Atlantic, indicating increased zonal mean SST gradient along the equatorial Atlantic. It allows the winter Atlantic-Niño and its relevant convection to be displaced to the west and to be enhanced by stronger thermocline feedback (Fig. 4b and Supplementary Figs. 10 and 11), similar to the frequent occurrence of CP-type El Niño events under La Niña-like mean state[49]. Thus, a stronger atmospheric teleconnection toward the Pacific is established, triggering ENSO events.

Meanwhile, the atmospheric responses over the tropical Pacific to the winter Atlantic-Niño during 1940–1975 are illustrated in Fig. 4b (Supplementary Figs. 8 and 9). These responses were first observed over the off-equatorial North Pacific (5–10°N) in winter (D[0]JF[1]), and later expanded both equatorward and poleward in spring. To comprehend the atmospheric response over the tropical Pacific to the Atlantic-Niño induced atmospheric teleconnection according to the different tropical Pacific mean state, we devised a vertical wind index (VWI). The VWI is defined by the areal average of upward motion (-omega at 500hPa) over the equatorial Pacific (150°E–120°W, 5°S–5°N) during DJF. It should be noted that the following results are not significantly influenced by minor variations in the chosen season or area.

Figure 6a, b show anomalous precipitation in JFM regressed onto VWI during the periods of 1940–1975 (*c.f.*, La Niña-like mean state) and 1980–2015 (*c.f.*, El Niño-like mean state), along with their differences (Fig. 6c). A 1-month lag was applied to account for the effect of vertical wind on precipitation. The analysis revealed that, under both equatorial Pacific warming and cooling mean states, anomalous vertical wind enhances precipitation over the equatorial Pacific (Fig. 6a, b). However, notable differences in precipitation response are observed over off-equatorial North Pacific (150°E–120°W, 5–10°N) between 1940–1975 and 1980–2015 (0.645 and −0.429 in Supplementary Table 2), indicating a greater sensitivity of precipitation response over the off-equatorial North Pacific during 1940–1975, attributable to the poleward-shifted Pacific ITCZ (Fig. 6c).

In addition, we conducted further analysis to examine how the sensitivity of precipitation to the VWI over the equatorial Pacific and over off-equatorial North Pacific is influenced by the variation of equatorial Pacific climatological SST (Supplementary Fig. 13). The results indicate the sensitivity of equatorial precipitation to the vertical wind is proportional to the climatological SST in the equatorial Pacific. Conversely, the sensitivity of north-off equatorial precipitation to the vertical wind is inversely proportional to the

climatological SST in the equatorial Pacific. These results imply that ITCZ location, controlled by climatological SST in the equatorial Pacific, determines the location of highest sensitivity for precipitation over the tropical Pacific.

In short, winter Atlantic Niño-induced signals are first observed in the off-equatorial North Pacific along the poleward-shifted ITCZ during 1940–1975 (Fig. 4a). Since atmospheric feedback processes in the subtropics are enhanced[50] when ITCZ is shifted poleward due to long-term variability (e.g., AMO or IPO)[51–53], significant signals can be widely observed from the tropics to the subtropics in spring. Consequently, ENSO can be developed not only by the Bjerknes feedback along the equator, but also by trade wind charging/discharging in connection with the subtropics[54–56].

Summer Atlantic-Niño effects on ENSO under eastern equatorial Pacific warming mean state (1980–2015)

During 1980–2015, the influence of the summer Atlantic-Niño on ENSO becomes significant via strong Walker circulation. Regarding this, it is worth noting that the signals induced by Atlantic-Niño events are primarily located along the equator in the Pacific. To examine the sensitivity of atmospheric responses to the summer Atlantic-Niño induced atmospheric teleconnection according to the climatological mean state in the Pacific, we again employed the VWI, at this moment in MAM, since the atmospheric teleconnection toward the Pacific begins in the season as the summer Atlantic-Niño develops (Fig. 2b and Supplementary Figs. 2 and 3).

Figure 6d–f show the anomalous precipitation along the equatorial Pacific in AMJ regressed on the VWI under the equatorial Pacific warming and cooling mean states, along with their difference. A one-month lag between VWI and precipitation is considered to account for the effect of vertical wind on precipitation. The precipitation response over the equatorial Pacific (150°E–120°W, 5°S–5°N) during 1980–2015 is greater than 1940–1975 (0.783 and 0.625, respectively; Supplementary Table 2) due to the equatorward shifted Pacific ITCZ. This result suggests that when the vertical wind over the equatorial Pacific occurs *via* modified Walker circulation induced by the summer Atlantic-Niño, the atmospheric response along the equator can be amplified during the equatorial Pacific warming mean state (Fig. 6f).

SALLJ and its connection to the summer Atlantic-Niño from an interdecadal perspective (1980–2015)

There is a connection between the SALLJ and the summer Atlantic-Niño during 1980–2015, whereas their connection is broken during 1940–1975. In this regard, we conducted an analysis to investigate the interannual connectivity between the SALLJ and summer Atlantic-Niño from the perspective of long-term modulation of the climatological mean state. During the period when the summer Atlantic-Niño leads ENSO (i.e., opposite phase of Fig. 5), the climatological mean SALLJ gets intensifies since its basic direction is northerly. The intensified northerly mean SALLJ coincides with a decreased climatological mean precipitation over the Atlantic ITCZ and South Atlantic Convergence Zone (SACZ), as well as an increased climatological mean precipitation over the La Plata basin in the southeastern South America. Thus, the stronger climatological northerly mean SALLJ can be possible as bridging the sinking motion over the tropical South America to the rising motion over the mid-latitude.

The decreased climatological mean precipitation over the tropical South America is attributed to the climatologically equatorial eastern Pacific warming and tropical western Atlantic cooling (opposite phase of Fig. 5)[57,58]. Previous study indicated that the climatological mean SALLJ tends to intensify under the AMO negative phases, and vice versa[59]. Additionally, it has been proposed that intensified climatological mean SALLJ is explained by the poleward-shifted South Atlantic Convergence Zone (SACZ) due to the poleward-shifted South Atlantic Subtropical High (around 10–50°W and 20–40°S)[60].

Based on the analysis, the meridionally extended interannual SALLJ during 1980–2015 can be formed under the climatological intensified northerly mean SALLJ. Then the interannual SALLJ links to the summer Atlantic-Niño, thereby facilitating the formation of strong convection and triggering atmospheric teleconnections.

DISCUSSION

The influence of Atlantic-Niños is not stationary but varies over decades. Specifically, the summer Atlantic-Niño effect on ENSO was more pronounced during the early and late twentieth century, whereas the winter Atlantic-Niño effect was dominant during the mid-twentieth century[29]. In this study, we examined spatiotemporal processes to understand how summer and winter Atlantic-Niño events initiate ENSO and investigated the role of the climatological mean state in these processes.

During the period when winter Atlantic-Niño leads ENSO with a lag of 1-year (e.g., 1940–1975), the equatorial Pacific exhibits a cold mean state, while the tropical western Atlantic has a warm mean state (Fig. 5). This configuration facilitates strong air–sea interactions over the tropical western Atlantic. As a result, the winter Atlantic-Niño can intensify and expand toward the tropical South America, thereby modulating atmospheric teleconnections toward the Pacific. Throughout this period, the atmospheric responses over the off-equatorial North Pacific were particularly sensitive, following the poleward-shifted Pacific ITCZ. In turn, the atmospheric teleconnection induced anomalous northeasterly trade winds over the off-equatorial North Pacific. These anomalous trade winds played a crucial role in charging and discharging equatorial heat content, providing favorable conditions for ENSO development. Simultaneously, atmospheric feedback processes relayed the easterly wind anomalies into the equatorial Pacific, initiating ENSO. This process suggests the relationship between winter Atlantic-Niño events and the North Pacific subtropical high. Comprehensively, winter Atlantic-Niño–ENSO connection seems to have some similarity with the seasonal footprinting mechanism[50,61,62], PMM[38,63,64], or NTA effect on ENSO[36,65,66].

During the period when summer Atlantic-Niño leads ENSO with a lag of half-year (e.g., 1980–2015), equatorial Pacific experiences a warming mean state while tropical western Atlantic exhibits a cold mean state. With the weakened zonal SST gradient along the equatorial Atlantic, the summer Atlantic-Niño gets weakened (Supplementary Figs. 10 and 11). However, during this period, the interannual SALLJ tends to meridionally extend under the stronger northerly mean SALLJ, which links to the summer Atlantic-Niño. Their combination effectively modulates the Walker circulation. Meanwhile, the atmospheric response is sensitive along the equatorial Pacific under the equatorward shifted Pacific ITCZ, enabling the ENSO events to develop fast by the direct development of equatorial Kelvin waves. Consequently, we conclude that the presence of strong and extensive convection over the Amazon to equatorial Atlantic, rather than the intensity of the Atlantic-Niño, is a pre-requisite for the connection between summer/winter Atlantic-Niño and ENSO. Our findings align with previous studies[30,31].

Until now, we try to view the distinct decadal modulation of the Atlantic-Niño and ENSO connection as a long-term natural variability, associated with the interdecadal modulation of Atlantic–South America–Pacific mean state. However, it is beneficial to acknowledge that South America has experienced warming due to the global warming[67]. The South America warming enhances the land-sea thermal contrast and increases the amount of available moisture, thereby intensifying the South America Monsoon and the SALLJ. Since we verified that the SALLJ connection to the Atlantic-Niño is possible under strong mean

SALLJ, we can expect the Atlantic-Niño's influence on ENSO can be stronger in future periods of global warming.

Although we have examined the interdecadal modulation of the lead time of the Atlantic-Niño effect on ENSO and the role of climatological mean states by analyzing observational reanalysis datasets, further verification using climate model simulation is necessary. However, most climate models face challenges in simulating the realistic basic state of the Atlantic and its interactions with other ocean basins[37,68,69]. Therefore, careful modeling approaches are required to increase our understanding of the influence of Atlantic-Niño on ENSO.

METHOD

Reanalysis dataset

The Extended Reconstruction Sea Surface Temperature version 5 (ERSSTv5) dataset was employed as the primary source of sea surface temperature (SST) data for this study. ERSSTv5 is a global monthly dataset derived from the International Comprehensive Ocean-Atmosphere Dataset (ICOADS) and can be accessed at https://www.esrl.noaa.gov/psd/data/data.php[70]. This dataset covers the period from 1854 to the present, making it suitable for investigating natural variability on interdecadal timescales. For the analysis of atmospheric processes, the 20th Century Reanalysis version 3 (20CRv3) datasets from the National Oceanic and Atmospheric Administration (NOAA) were utilized. These monthly datasets span from 1836 to 2015[71], providing a sufficiently long time period to examine interdecadal variability of climate phenomena. Prior to conducting the analysis, all datasets were detrended for the period under investigation.

Index

In order to investigate the strength of the Atlantic Niño effect on ENSO, monthly Atlantic-Niño and ENSO indices were defined. ENSO is represented by SSTA averaged over the Niño-3.4 region (120°W–170°W and 5°S–5°N) and the Atlantic-Niño index is obtained from the areally averaged SSTA over 0°–20°W and 5°S–5°N. The latitudinal range of the Atlantic-Niño index is set to be the same as that of ENSO. Although this is slightly wider than the conventional range (3°S–3°N), it does not significantly change the results. We defined the summer/winter Atlantic-Niño index by averaging the monthly Atlantic-Niño during June–July–August (JJA) and December–January–February (DJF), respectively. For the summer Atlantic-Niño, the previous winter (DJF) ENSO signal was removed linearly using linear regression analysis against the ENSO index in order to exclude previous winter ENSO effects. For the winter Atlantic-Niño index, simultaneous winter (DJF) ENSO signals were removed. The effects of ENSO signal removal are negligible since the correlation between the previous winter ENSO and the following Atlantic-Niño indices are insignificant (Fig. 1a). The South America low-level jet (SALLJ) index was obtained by averaging meridional wind at 850 hPa over 55°–65°W and 15°–25°S, and the Subtropical North Pacific high index was obtained by averaging the SLPA over 120°–180°W and 5°–30°N.

DATA AVAILABILITY

ERSSTv5 and 20CRv3 can be downloaded from following URL, https://psl.noaa.gov/data/gridded/data.noaa.ersst.v5.html and https://psl.noaa.gov/data/gridded/data.20thC_ReanV3.html, respectively.

CODE AVAILABILITY

Codes used in the manuscript are available upon reasonable requests from J.-H.P. (jhp11010@gmail.com).

Received: 12 February 2023; Accepted: 17 July 2023;
Published online: 29 July 2023

REFERENCES

1. Folland, C. K., Colman, A. W., Rowell, D. P. & Davey, M. K. Predictability of Northeast Brazil Rainfall And Real-time Forecast Skill, 1987–98. *J. Clim.* **14**, 1937–1958 (2001).
2. Okumura, Y. & Xie, S.-P. Interaction of the Atlantic equatorial cold tongue and the african monsoon. *J. Clim.* **17**, 3589–3602 (2004).
3. Rodríguez-Fonseca, B. et al. Variability and predictability of west african droughts: a review on the role of sea surface temperature anomalies. *J. Clim.* **28**, 4034–4060 (2015).
4. Cassou, C., Deser, C., Terray, L., Hurrell, J. W. & Drévillon, M. Summer sea surface temperature conditions in the North Atlantic and their impact upon the atmospheric circulation in early winter. *J. Clim.* **17**, 3349–3363 (2004).
5. Kucharski, F. et al. A Gill–Matsuno-type mechanism explains the tropical Atlantic influence on African and Indian monsoon rainfall. *Q. J. R. Meteorol. Soc.* **135**, 569–579 (2009).
6. Kucharski, F., Bracco, A., Yoo, J. H. & Molteni, F. Atlantic forced component of the Indian monsoon interannual variability. *Geophys. Res. Lett.* **35**, L04706 (2008).
7. García-Serrano, J., Losada, T., Rodríguez-Fonseca, B. & Polo, I. Tropical Atlantic Variability Modes (1979–2002). Part II: time-evolving atmospheric circulation related to SST-forced tropical convection. *J. Clim.* **21**, 6476–6497 (2008).
8. Carton, J. A. & Huang, B. Warm events in the tropical Alantic. *J. Phys. Oceanogr.* **24**, 888–903 (1994).
9. Xie, S.-P. & Carton, J. A. Tropical Atlantic variability: patterns, mechanisms, and impacts. *Am. Geophys. Union Geophys. Monogr. Ser.* **147**, 121–142 (2004).
10. Keenlyside, N. S. & Latif, M. Understanding equatorial Atlantic interannual variability. *J. Clim.* **20**, 131–142 (2007).
11. Lübbecke, J. F. et al. Equatorial Atlantic variability—modes, mechanisms, and global teleconnections. *WIREs Clim. Change* **9**, e527 (2018).
12. Polo, I., Rodríguez-Fonseca, B., Losada, T. & García-Serrano, J. Tropical atlantic variability modes (1979-2002). Part I: time-evolving SST modes related to West African rainfall. *J. Clim.* **21**, 6457–6475 (2008).
13. Bjerknes, J. Atmospheric teleconnections from the equatorial Pacific. *Mon. Weather Rev.* **97**, 163–172 (1969).
14. Zebiak, S. E. Air–sea interaction in the equatorial atlantic region. *J. Clim.* **6**, 1567–1586 (1993).
15. Lübbecke, J. F., Böning, C. W., Keenlyside, N. S. & Xie, S.-P. On the connection between Benguela and equatorial Atlantic Niños and the role of the South Atlantic Anticyclone. *J. Geophys. Res. Ocean.* **115**, C09015 (2010).
16. Richter, I. et al. On the triggering of Benguela Niños: remote equatorial versus local influences. *Geophys. Res. Lett.* **37**, L20604 (2010).
17. Richter, I. et al. Multiple causes of interannual sea surface temperature variability in the equatorial Atlantic Ocean. *Nat. Geosci.* **6**, 43–47 (2013).
18. Ham, Y. G. et al. Inter-basin interaction between variability in the South Atlantic Ocean and the El Niño/Southern Oscillation. *Geophys. Res. Lett.* **48**, 1–11 (2021).
19. Zhang, L. & Han, W. Indian Ocean Dipole leads to Atlantic Niño. *Nat. Commun.* **12**, 5952 (2021).
20. Richter, I. et al. Phase locking of equatorial Atlantic variability through the seasonal migration of the ITCZ. *Clim. Dyn.* **48**, 3615–3629 (2017).
21. Kim, S.-K. & An, S.-I. Seasonal gap theory for ENSO phase locking. *J. Clim.* **34**, 5621–5634 (2021).
22. Wang, C. An overlooked feature of tropical climate: Inter-Pacific-Atlantic variability. *Geophys. Res. Lett.* **33**, 1–5 (2006).
23. Rodríguez-Fonseca, B. et al. Are Atlantic Niños enhancing Pacific ENSO events in recent decades? *Geophys. Res. Lett.* **36**, L20705 (2009).
24. Ding, H., Keenlyside, N. S. & Latif, M. Impact of the Equatorial Atlantic on the El Niño Southern Oscillation. *Clim. Dyn.* **38**, 1965–1972 (2012).
25. Kucharski, F., Kang, I.-S., Farneti, R. & Feudale, L. Tropical Pacific response to 20th century Atlantic warming. *Geophys. Res. Lett.* **38**, L03702 (2011).
26. Kucharski, F., Syed, F. S., Burhan, A., Farah, I. & Gohar, A. Tropical Atlantic influence on Pacific variability and mean state in the twentieth century in observations and CMIP5. *Clim. Dyn.* **44**, 881–896 (2015).
27. Polo, I., Martin-Rey, M., Rodriguez-Fonseca, B., Kucharski, F. & Mechoso, C. R. Processes in the Pacific La Niña onset triggered by the Atlantic Niño. *Clim. Dyn.* **44**, 115–131 (2015).
28. Okumura, Y. & Xie, S.-P. Some overlooked features of tropical Atlantic climate leading to a new Niño-like phenomenon. *J. Clim.* **19**, 5859–5874 (2006).
29. Hounsou-Gbo, A. et al. Summer and winter Atlantic Niño: connections with ENSO and implications. *Clim. Dyn.* **55**, 2939–2956 (2020).
30. Losada, T. & Rodríguez-Fonseca, B. Tropical atmospheric response to decadal changes in the Atlantic Equatorial Mode. *Clim. Dyn.* **47**, 1211–1224 (2016).

31. Losada, T., Rodríguez-Fonseca, B., Roberto Mechoso, C., Mohino, E. & Castaño-Tierno, A. Changes in interannual tropical Atlantic–Pacific basin interactions modulated by a South Atlantic Cooling. *J. Clim.* **35**, 4403–4416 (2022).
32. Martín-Rey, M., Polo, I., Rodríguez-Fonseca, B., Losada, T. & Lazar, A. Is there evidence of changes in tropical atlantic variability modes under AMO phases in the observational record? *J. Clim.* **31**, 515–536 (2018).
33. Martín-Rey, M., Rodríguez-Fonseca, B., Polo, I. & Kucharski, F. On the Atlantic–Pacific Niños connection: a multidecadal modulated mode. *Clim. Dyn.* **43**, 3163–3178 (2014).
34. Rodríguez-Fonseca, B. et al. *Interacting Climates of Ocean Basins: Observations, Mechanisms, Predictability, and Impacts* (ed. Mechoso, C. R.) p. 120–152 (Cambridge University Press, 2020).
35. Barreiro, M. & Tippmann, A. Atlantic modulation of El Niño influence on summertime rainfall over southeastern South America. *Geophys. Res. Lett.* **35**, 1–5 (2008).
36. Wang, L., Yu, J. Y. & Paek, H. Enhanced biennial variability in the Pacific due to Atlantic capacitor effect. *Nat. Commun.* **8**, 14887 (2017).
37. Park, J. H. et al. Two regimes of inter-basin interactions between the Atlantic and Pacific Oceans on interannual timescales. *npj Clim. Atmos. Sci.* **6**, 1–8 (2023).
38. Park, J. H., Li, T., Yeh, S. W. & Kim, H. Effect of recent Atlantic warming in strengthening Atlantic–Pacific teleconnection on interannual timescale via enhanced connection with the pacific meridional mode. *Clim. Dyn.* **53**, 371–387 (2019).
39. Chang, P., Fang, Y., Saravanan, R., Ji, L. & Seidel, H. The cause of the fragile relationship between the Pacific El Nïo and the Atlantic Nïo. *Nature* **443**, 324–328 (2006).
40. Lübbecke, J. F. & McPhaden, M. J. On the inconsistent relationship between Pacific and Atlantic Niños. *J. Clim.* **25**, 4294–4303 (2012).
41. Jiang, L. & Li, T. Impacts of Tropical North Atlantic and Equatorial Atlantic SST anomalies on ENSO. *J. Clim*. https://doi.org/10.1175/JCLI-D-20-0835.1 (2021).
42. Rodrigues, R. R., Campos, E. J. D. & Haarsma, R. The impact of ENSO on the South Atlantic subtropical dipole mode. *J. Clim.* **28**, 2691–2705 (2015).
43. Ham, Y.-G. et al. Inter-basin interaction between variability in the South Atlantic Ocean and the El Niño/Southern Oscillation. *Geophys. Res. Lett.* **48**, e2021GL093338 (2021).
44. Montini, T. L., Jones, C. & Carvalho, L. M. V. The South American low-level jet: a new climatology, variability, and changes. *J. Geophys. Res. Atmos.* **124**, 1200–1218 (2019).
45. Jones, C. Recent changes in the South America low-level jet. *npj Clim. Atmos. Sci.* **2**, 20 (2019).
46. Kug, J. S. & Jin, F. F. Two types of El Niño events: cold tongue El Niño and warm pool El Niño. *J. Clim.* **22**, 1499–1515 (2009).
47. Ashok, K., Behera, S. K., Rao, S. A., Weng, H. & Yamagata, T. El Niño Modoki and its possible teleconnection. *J. Geophys. Res. Ocean.* **112**, 1–27 (2007).
48. Kao, H. Y. & Yu, J. Y. Contrasting Eastern-Pacific and Central-Pacific types of ENSO. *J. Clim.* **22**, 615–632 (2009).
49. Chung, P. H. & Li, T. Interdecadal relationship between the mean state and El Niño types. *J. Clim.* **26**, 361–379 (2013).
50. Park, J.-H. et al. Role of the climatological intertropical convergence zone in the seasonal footprinting mechanism of El Niño–Southern Oscillation. *J. Clim.* **34**, 5243–5256 (2021).
51. Knight, J. R., Folland, C. K. & Scaife, A. A. Climate impacts of the Atlantic multidecadal oscillation. *Geophys. Res. Lett.* **33**, 2–5 (2006).
52. Levine, A. F. Z., Frierson, D. M. W. & McPhaden, M. J. AMO forcing of multidecadal pacific ITCZ variability. *J. Clim.* **31**, 5749–5764 (2018).
53. Power, S., Casey, T., Folland, C., Colman, A. & Mehta, V. Inter-decadal modulation of the impact of ENSO on Australia. *Clim. Dyn.* **15**, 319–324 (1999).
54. Anderson, B. T., Perez, R. C. & Karspeck, A. Triggering of El Niño onset through trade wind-induced charging of the equatorial Pacific. *Geophys. Res. Lett.* **40**, 1212–1216 (2013).
55. Anderson, B. T. & Perez, R. C. ENSO and non-ENSO induced charging and discharging of the equatorial Pacific. *Clim. Dyn.* **45**, 2309–2327 (2015).
56. Chakravorty, S. et al. Testing the trade wind charging mechanism and its influence on ENSO variability. *J. Clim.* **33**, 7391–7411 (2020).
57. Friedman, A. R., Bollasina, M. A., Gastineau, G. & Khodri, M. Increased Amazon Basin wet-season precipitation and river discharge since the early 1990s driven by tropical Pacific variability. *Environ. Res. Lett.* **16**, 034033 (2021).
58. Wang, X. Y., Li, X., Zhu, J. & Tanajura, C. A. S. The strengthening of Amazonian precipitation during the wet season driven by tropical sea surface temperature forcing. *Environ. Res. Lett.* **13**, 094015 (2018).
59. Jones, C. & Carvalho, L. M. V. The influence of the Atlantic multidecadal oscillation on the eastern Andes low-level jet and precipitation in South America. *npj Clim. Atmos. Sci.* **1**, 1–7 (2018).
60. Zilli, M. T., Carvalho, L. M. V. & Lintner, B. R. The poleward shift of South Atlantic Convergence Zone in recent decades. *Clim. Dyn.* **52**, 2545–2563 (2019).
61. Vimont, D. J., Battisti, D. S. & Hirst, A. C. The seasonal footprinting mechanism in the CSIRO general circulation models*. *J. Clim.* **16**, 2653–2667 (2003).
62. Vimont, D. J., Battisti, D. S. & Hirst, A. C. Footprinting: a seasonal connection between the tropics and mid-latitudes. *Geophys. Res. Lett.* **28**, 3923–3926 (2001).
63. Chiang, J. C. H. & Vimont, D. J. Analogous Pacific and Atlantic Meridional Modes of tropical atmosphere–ocean variability. *J. Clim.* **17**, 4143–4158 (2004).
64. Park, J. H., Kug, J. S., Li, T. & Behera, S. K. Predicting El Niño beyond 1-year lead: effect of the Western Hemisphere Warm Pool. *Sci. Rep.* **8**, 1–8 (2018).
65. Park, J.-H. et al. Role of the climatological North Pacific High in the North Tropical Atlantic–ENSO Connection. *J. Clim.* **35**, 3215–3226 (2022).
66. Ham, Y. G., Kug, J. S., Park, J. Y. & Jin, F. F. Sea surface temperature in the north tropical Atlantic as a trigger for El Niño/Southern Oscillation events. *Nat. Geosci.* **6**, 112–116 (2013).
67. de Barros Soares, D., Lee, H., Loikith, P. C., Barkhordarian, A. & Mechoso, C. R. Can significant trends be detected in surface air temperature and precipitation over South America in recent decades? *Int. J. Climatol.* **37**, 1483–1493 (2017).
68. Richter, I., Xie, S. P., Behera, S. K., Doi, T. & Masumoto, Y. Equatorial Atlantic variability and its relation to mean state biases in CMIP5. *Clim. Dyn.* **42**, 171–188 (2014).
69. Wang, C., Zhang, L., Lee, S. K., Wu, L. & Mechoso, C. R. A global perspective on CMIP5 climate model biases. *Nat. Clim. Change* **4**, 201–205 (2014).
70. Huang, B. et al. Extended reconstructed sea surface temperature, version 5 (ERSSTv5): upgrades, validations, and intercomparisons. *J. Clim.* **30**, 8179–8205 (2017).
71. Slivinski, L. C. et al. Towards a more reliable historical reanalysis: Improvements for version 3 of the twentieth century Reanalysis system. *Q. J. R. Meteorol. Soc.* **145**, 2876–2908 (2019).

ACKNOWLEDGEMENTS

We are grateful for the valuable comments and suggestions offered by the anonymous reviewers and editors. J.-H.P. was supported by the National Research Foundation of Korea (NRF) grant funded by the Korea government (MSIT) (NRF-2023R1A2C1004083 and RS-2023-00219830). J.-S.K. was supported by the National Research Foundation of Korea (NRF) grant funded by the Korean government (NRF-2022R1A3B1077622). Y.-M.Y. was funded by the Korea Meteorological Administration Research and Development Program under Grant (KMI2022-01110). M.-K.S. was supported by Korea Environmental Industry & Technology Institute (KEITI) through "Project for developing an observation-based GHG emissions geospatial information map", funded by Korea Ministry of Environment (MOE)(RS-2023-00232066). H.-J.K. was supported by Low-Carbon and Climate Impact Research Centre at the School of Energy and Environment, City University of Hong Kong and CityU Start-up Grant for New Faculty (No. 9610581). S.-I.A. was supported by the National Research Foundation of Korea (NRF) grant funded by the Korean government (NRF-2018R1A5A1024958).

AUTHOR CONTRIBUTIONS

J.-H.P. conceived the idea and shared it with other coauthors. J.-H.P. conducted the analyses and prepare the figures together with H.-J.P. The manuscript was written by J.-H.P. and J.-S.K. All the authors participated in discussions on the results and reviewed the manuscript.

COMPETING INTERESTS

The authors declare no competing interests.

ADDITIONAL INFORMATION

Supplementary information The online version contains supplementary material available at https://doi.org/10.1038/s41612-023-00429-9.

Correspondence and requests for materials should be addressed to Jae-Heung Park or Jong-Seong Kug.

Reprints and permission information is available at http://www.nature.com/reprints

Publisher's note Springer Nature remains neutral with regard to jurisdictional claims in published maps and institutional affiliations.